nature neuroscience

Focal transplantation–based astrocyte replacement is neuroprotective in a model of motor neuron disease

Angelo C Lepore[1], Britta Rauck[1], Christine Dejea[1], Andrea C Pardo[1], Mahendra S Rao[2], Jeffrey D Rothstein[1,3] & Nicholas J Maragakis[1]

Cellular abnormalities in amyotrophic lateral sclerosis (ALS) are not limited to motor neurons. Astrocyte dysfunction also occurs in human ALS and transgenic rodents expressing mutant human SOD1 protein ($SOD1^{G93A}$). Here we investigated focal enrichment of normal astrocytes using transplantation of lineage-restricted astrocyte precursors, called glial-restricted precursors (GRPs). We transplanted GRPs around cervical spinal cord respiratory motor neuron pools, the principal cells whose dysfunction precipitates death in ALS. GRPs survived in diseased tissue, differentiated efficiently into astrocytes and reduced microgliosis in the cervical spinal cords of $SOD1^{G93A}$ rats. GRPs also extended survival and disease duration, attenuated motor neuron loss and slowed declines in forelimb motor and respiratory physiological functions. Neuroprotection was mediated in part by the primary astrocyte glutamate transporter GLT1. These findings indicate the feasibility and efficacy of transplantation-based astrocyte replacement and show that targeted multisegmental cell delivery to the cervical spinal cord is a promising therapeutic strategy for slowing focal motor neuron loss associated with ALS.

ALS, a motor neuron disorder that affects ~30,000 individuals in the United States alone, is characterized by a relatively rapid degeneration of upper and lower motor neurons, with death from respiratory failure normally occurring 2–5 years after diagnosis[1]. The vast majority of cases are sporadic, but 5–10% are familial, with 20% of those linked to mutations in the Cu/Zn superoxide dismutase 1 (*SOD1*) gene[2]. Transgenic mice[3–5] and rats[6] carrying mutant human *SOD1* genes (resulting in amino acid substitutions G93A, G37R and G85R) recapitulate many features of the human disease.

Despite the relative selectivity of motor neuron cell death, animal and tissue culture models of familial ALS suggest that non-neuronal cells contribute significantly to neuronal dysfunction and death[7–13]. CNS astrocytes outnumber their neuronal counterparts approximately tenfold and have crucial roles in adult CNS homeostasis[14], including the vast majority of synaptic glutamate uptake[15,16], maintenance of extracellular potassium and nutrient support of neurons. Multiple properties of spinal cord and brain astrocytes are compromised in ALS, and these changes often precede clinical disease onset[17]. Initial evidence for an astroglial contribution to ALS came from studies of humans and rodent ALS models indicating dysfunction and large decreases in levels of the primary astrocyte glutamate transporter, GLT1 (EAAT2 in human), in areas of motor neuron loss[6,18]. Confirmation of a role for non-neuronal cells came from recent studies of chimeric animals indicating that glia can modulate mutant SOD1-induced pathological changes in neighboring motor neurons[8]. These studies highlight the important role of astrocyte–motor neuron interactions in the etiology of ALS.

Regardless of whether astrocyte dysfunction is the cause of disease or a consequence of neuronal death, altered physiology of pathologic astrocytes results in further susceptibility to motor neuron loss and contributes to disease progression. We hypothesized that replacement or enrichment with healthy astrocytes, using transplantation of GRPs[19,20]—lineage-restricted astrocyte precursors derived from developing spinal cord—could be a therapeutic approach for slowing or halting the disease course. Such an approach would lend itself to reconstituting a more normal astrocytic environment in the spinal cord. This may include, for example, restoration of extracellular glutamate homeostasis by preventing ALS-associated loss of GLT1. Patients with ALS (and animals with mutant SOD1) ultimately succumb to disease because of respiratory compromise resulting from loss of phrenic motor neuron innervation of the diaphragm[21,22]. To target therapy to diaphragmatic function, we transplanted GRPs into cervical spinal cord ventral gray matter of transgenic rats expressing mutant human SOD1 protein ($SOD1^{G93A}$ rats). Because this approach is aimed at neuroprotection rather than neuronal replacement, reconstitution of spinal cord astrocytes may be a valuable approach to cellular-based therapeutics.

RESULTS

To assess the effects of GRP transplantation, we transplanted GRPs into the cervical spinal cords of 90-d-old $SOD1^{G93A}$ rats. Because loss of

[1]Department of Neurology, Johns Hopkins University School of Medicine, 600 N. Wolfe Street, Meyer 6-119, Baltimore, Maryland 21287, USA. [2]Invitrogen Corporation, 1610 Faraday Avenue, Carlsbad, California, USA. [3]Department of Neuroscience, The Johns Hopkins University School of Medicine, 600 N. Wolfe St., Meyer 6-109, Baltimore, Maryland 21287, USA. Correspondence should be addressed to N.J.M. (nmaragak@jhmi.edu).

Received 31 July; accepted 11 September; published online 19 October 2008; doi:10.1038/nn.2210

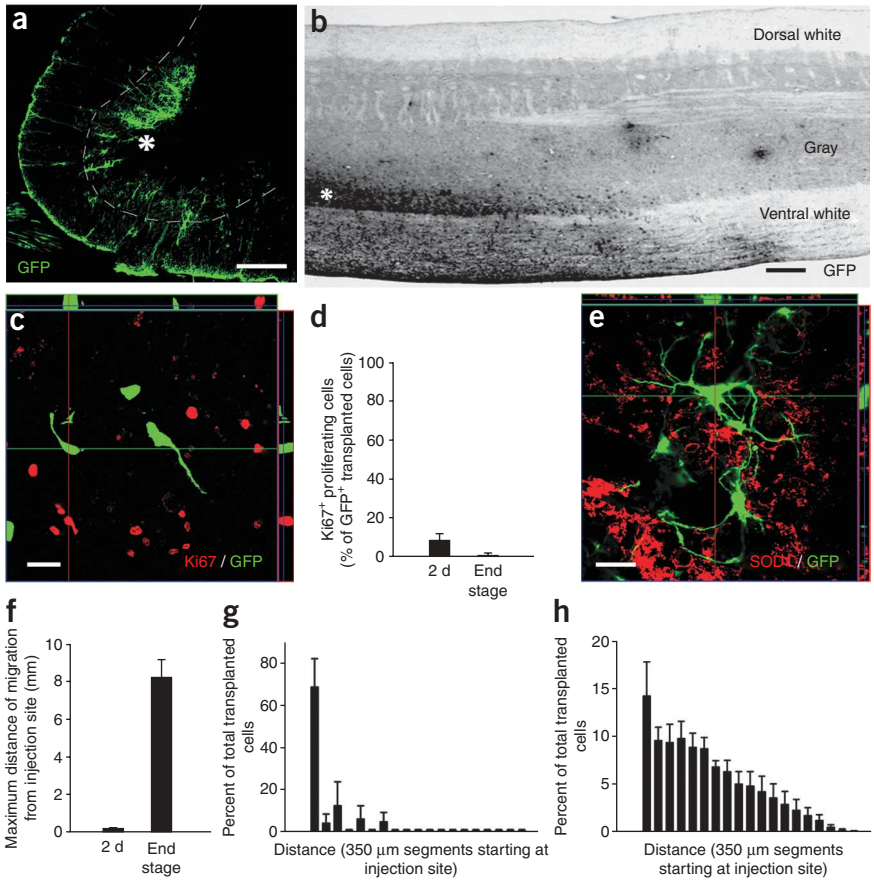

Figure 1 GRP transplants robustly survived and migrated in the cervical spinal cords of SOD1^{G93A} rats. (**a**,**b**) GRP transplants robustly survived in gray (**a**,**b**) and white (**b**) matter regions of the cervical spinal cord at disease end stage. Transplants were located in both ventral gray matter (**a**,**b**) and surrounding white matter (**b**) regions at sites of injection (*) and migrated away from injection sites in both rostral and caudal directions along white-matter tracts (**b**). (**c**) The vast majority of transplanted cells did not express the proliferation marker Ki67 *in vivo* 2 d after transplantation. (**d**) Quantification confirmed that only a small percentage of GFP$^+$ cells expressed Ki67 2 d after transplantation, and no transplant proliferation occurred at disease end stage. (**e**) GFP$^+$ transplants did not fuse with host human SOD1$^+$ cells. (**f**) Quantification of GRP migration revealed that 2 d after engraftment, transplanted cells were found on average no farther than 0.19 mm from the injection site; at disease end stage, GRPs had migrated up to 8.3 mm from the injection site. (**g**,**h**) Percentage of cells at various distances from injection sites. The migratory patterns of transplants in gray versus white matter were distinct. The vast majority of cells were located close to the injection site in gray matter (**g**). In white matter, the highest proportion of cells was located close to the injection site, and the numbers of cells gradually tapered away with increased distance (**h**). Scale bars, 200 μm (**a**,**b**) or 20 μm (**c**,**e**). Error bars indicate s.e.m.

diaphragm function is the primary cause of death in ALS patients and rodent models[21,22], we targeted the respiratory motor neurons innervating the diaphragm for transplantation using bilateral cell injections at cervical spinal cord levels 4, 5 and 6.

Robust transplant survival in SOD1^{G93A} cervical spinal cord

We transplanted green fluorescent protein (GFP)-positive GRPs into the cervical spinal cords of SOD1^{G93A} rats ($n = 34$) at 90 d of age. Despite ongoing disease progression, GRPs robustly survived in gray (**Fig. 1a**,**b**) and white (**Fig. 1b**) matter regions of the cervical spinal cord at disease end stage, up to 80 d after transplantation. We grafted a total of 9.0×10^5 cells (1.5×10^5 cells at each of six sites) into each rat and found six discrete sites with transplanted cells in each rat. Quantification of GFP$^+$ GRPs at end stage revealed that 32.2 ± 4.6% of transplanted cells survived ($n = 3$). No damage to the spinal cord, including cyst formation, was detected when spinal cords from any of the groups (injection with media, dead cells, fibroblasts or GRPs) were assessed with cresyl violet staining (data not shown), and no sign of tumor formation was found in any rat (see **Supplementary Methods** online).

We next profiled graft proliferation by immunohistochemical analysis of GFP and the proliferation marker Ki67 (**Fig. 1c** and **Supplementary Methods**). Only a small percentage of cells continued to divide 2 d after transplantation (8.1 ± 2.1%; $n = 3$), and transplant-derived cells no longer proliferated at disease end stage (0.6 ± 0.6%; $n = 3$; **Fig. 1d**). These results suggest that the robust survival of transplanted cells at disease end stage was not a function of extensive early graft proliferation *in vivo*.

To assess whether transplantation of greater numbers of cells would result in enhanced graft survival, we delivered nearly three-fold more cells (4.0×10^5 cells) to each site; however, this approach resulted in obvious necrotic tissue damage at the sites of injection.

No instances of GFP$^+$ transplanted cells colabeled with human SOD1 were ever noted at disease end stage, indicating that transplanted GFP$^+$ cells did not fuse with host cells (**Fig. 1e** and **Supplementary Methods**).

Ventral horn localization and white-matter migration

GRPs were specifically detected in the ventral horn (**Fig. 1a**), the region of ongoing degeneration. In addition, transplanted cells migrated extensively and selectively along surrounding white-matter tracts in both rostral and caudal directions (**Fig. 1b**). Quantification of migration revealed that 2 d after engraftment, transplanted cells were found on average no farther than 0.19 ± 0.03 mm from the injection site ($n = 4$; **Fig. 1f**), whereas they had migrated up to 8.3 ± 0.95 mm from the injection site at disease end stage ($n = 4$).

The migratory pattern of transplanted cells in gray versus white matter was distinct: the vast majority of cells were located close to the injection site in gray matter (**Fig. 1g**), whereas in white matter, the highest proportion of cells was located close to the injection site, but the numbers of cells gradually tapered away with increased distance (**Fig. 1h**). Even though widely dispersed, the majority of transplanted cells remained adjacent to the injection sites in both white and gray matter regions of the cervical spinal cord and were not seen in more distant brain or spinal cord regions (data not shown and **Supplementary Methods**).

Efficient astrocyte differentiation

We assessed the differentiation of transplanted cells by immunohistochemical analysis of GFP and specific markers of cell fate. Initially after

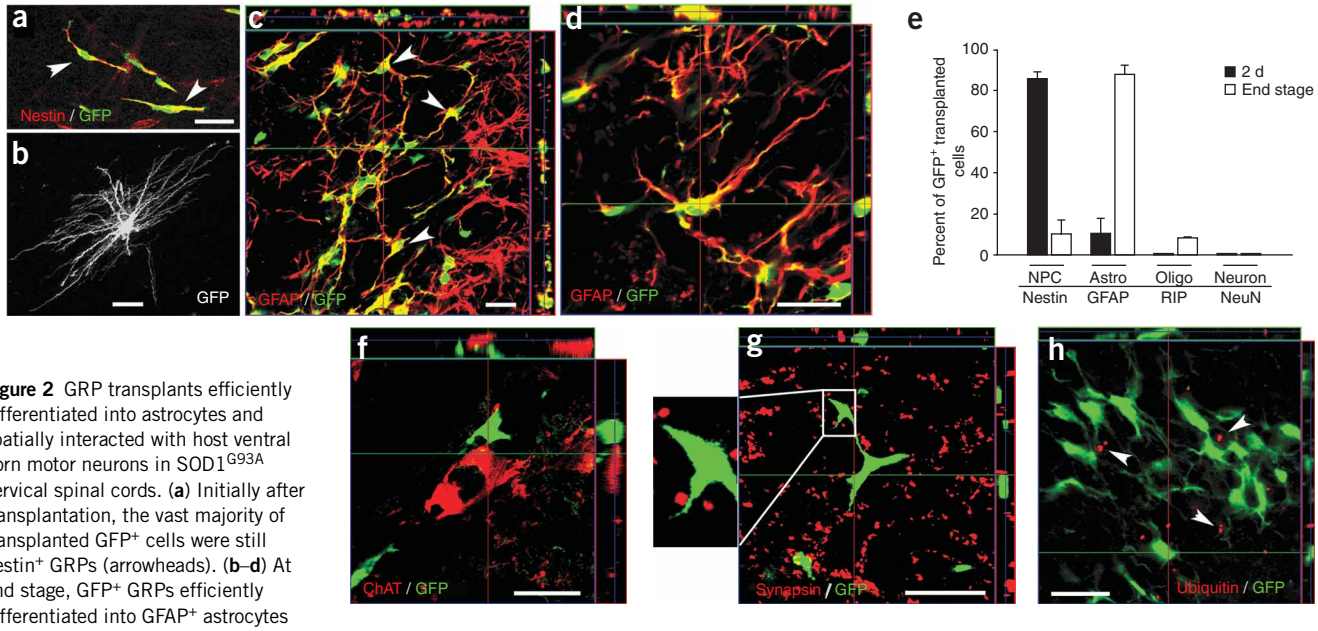

Figure 2 GRP transplants efficiently differentiated into astrocytes and spatially interacted with host ventral horn motor neurons in SOD1^{G93A} cervical spinal cords. (**a**) Initially after transplantation, the vast majority of transplanted GFP$^+$ cells were still nestin$^+$ GRPs (arrowheads). (**b**–**d**) At end stage, GFP$^+$ GRPs efficiently differentiated into GFAP$^+$ astrocytes after transplantation (**c**,**d**) and showed mature astrocytic morphologies (**b**). (**e**) Quantification of the differentiation profile of transplanted GRPs 2 d after transplantation and at disease end stage shows the efficient transition from immature to mature phenotypes *in vivo*. NPC, neural progenitor cells; Astro, astrocytes; Oligo, oligodendrocytes; RIP, oligodendrocyte marker; NeuN, neuronal marker. (**f**–**h**) Transplanted GFP$^+$ cells came into close direct contact with cell bodies of host ChAT$^+$ motor neurons (**f**) and with synapsin-positive synaptic sites (**g**; inset shows higher magnification) in the ventral horn. Extensive ubiquitin deposition (arrowheads) was found in host cervical spinal cord cells at disease end stage (**h**). However, only rare transplanted GFP$^+$ cells contained such ubiquitin aggregates, suggesting that transplanted cells did not succumb to a similar pathological fate as host astrocytes in response to disease. Scale bars, 25 μm. Error bars indicate s.e.m.

grafting, the vast majority of cells were still nestin$^+$ GRPs (85.4 ± 3.6%; **Fig. 2a**), with a small percentage of astrocytes constituting the remaining population (10.6 ± 7.5%). During the course of disease, graft-derived astrocytes assumed mature astrocyte morphologies (**Fig. 2b**). At end stage, transplanted GRPs had efficiently differentiated into glial fibrillary acidic protein (GFAP)-positive astrocytes (87.9 ± 4.0%; **Fig. 2c**,**d**). Quantification of the differentiation of transplanted GRPs 2 d after transplantation and at disease end stage revealed an efficient transition from immature to mature phenotypes *in vivo* ($n = 3$; **Fig. 2e**). A small percentage of cells also differentiated into oligodendrocytes by end stage (8.6 ± 0.35%). No transplanted cells gave rise to unexpected phenotypes such as neurons, microglia or macrophages. In addition, only a small percentage of cells remained as undifferentiated nestin$^+$ GRPs at end stage (10.2 ± 6.9%), indicating that the majority of transplanted cells differentiated into mature phenotypes (**Supplementary Methods**).

These cells not only localized in the vicinity of host motor neurons in the ventral horn, but also spatially interacted with host motor neuron soma and dendritic fields. Confocal microscopy revealed that transplanted GRPs were closely apposed to cell bodies of choline acetyltransferase (ChAT)-positive host motor neurons (**Fig. 2f**). We observed these interactions by three-dimensional reconstruction of confocal images showing GFP$^+$ cells surrounding host ChAT$^+$ motor neurons (**Supplementary Video 1** online). Confocal imaging of GFP and the presynaptic marker synapsin also showed the localization of transplanted GFP$^+$ cells at synaptic sites in the ventral gray matter (**Fig. 2g** and **Supplementary Methods**).

To determine whether transplanted cells succumb to a similar pathological fate as host astrocytes in response to disease, we examined two characteristic pathological changes observed in host astrocytes in the spinal cords of SOD1^{G93A} rats: the presence of ubiquitinated inclusions[3,5] and the loss of GLT1 expression[6]. We found extensive ubiquitin deposition in host cervical spinal cord motor neurons and astrocytes (data not shown). In contrast, as shown by confocal microscopy, the vast majority of transplanted GRP-derived cells at end stage did not contain ubiquitin aggregates (**Fig. 2h**); only 6.1 ± 1.7% of GFP$^+$ cells contained such inclusions ($n = 5$). In addition, grafted cells continued to express the astrocyte glutamate transporter protein GLT1 at end stage (**Supplementary Methods**).

Delayed decline in motor function and survival extension

SOD1^{G93A} rats show a typical pattern of disease progression in which onset of disease in hindlimbs precedes that in forelimbs, followed by end stage as a result of compromised respiratory function[23]. We delivered transplant cells to the cervical spinal cord to focally targeting forelimb and respiratory function, but not hindlimb motor neurons.

We first assessed whether delivery of transplanted cells to respiratory motor neurons could extend survival in SOD1^{G93A} rats. Compared to rats injected with medium ($n = 10$) and dead cell ($n = 7$) controls, rats transplanted with GRPs ($n = 10$) survived 16.9 d longer overall (medium, 155.8 ± 12.0 d overall survival; dead cells, 155.8 ± 14.0 d; GRPs, 172.7 ± 14.1 d; $P < 0.05$ for media versus GRPs; $P < 0.01$ for dead cells versus GRPs; **Fig. 3a**).

No effect of GRPs on hindlimb disease onset was noted (medium, 143.6 ± 12.3 d of age; dead cells, 142.2 ± 12.2 d; GRPs, 147.6 ± 12.9 d; $P > 0.05$; **Fig. 3b**). GRP-transplanted animals showed a trend, though not significant, toward delayed forelimb disease onset (medium, 151.0 ± 12.0 d of age; dead cells, 149.3 ± 13.2 d; GRPs, 162.6 ± 11.9; $P > 0.05$; **Fig. 3c**).

We also assessed the ability of transplant cells to delay the regional progression of disease. GRPs significantly delayed disease duration: the time between overall disease onset (hindlimb onset) and end stage

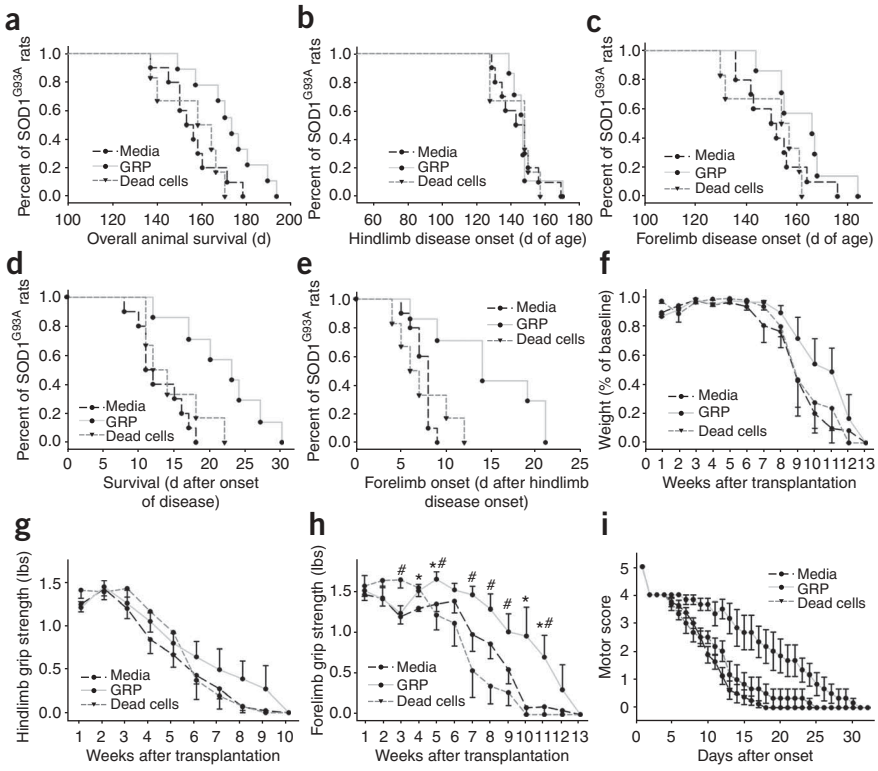

Figure 3 After transplantation into the cervical spinal cords of SOD1^{G93A} rats, transplanted GRPs extended survival and disease duration and slowed declines in forelimb grip strength and motor performance. (**a**) Compared to injection of media or dead cells, transplanted GRPs significantly increased overall rat survival. (**b**,**c**) GRPs had no effect on hindlimb disease onset (**b**) but promoted a trend toward delayed forelimb onset (**c**). (**d**) Survival after disease onset was significantly prolonged by GRPs. (**e**) A significant delay to forelimb disease onset after hindlimb onset was observed in GRP-transplanted rats. (**f**) GRPs did not significantly delay weight decline. (**g**,**h**) GRPs significantly delayed decline in forelimb grip strength (**h**; *, media versus GRPs; #, dead cells versus GRPs) but had no effect on the rate of decline of hindlimb grip strength decline (**g**). (**i**) GRPs also slowed the decline in motor performance. Error bars indicate s.e.m.

(medium, 12.9 ± 3.3 d; dead cells, 14.7 ± 4.5 d; GRPs, 21.9 ± 6.1 d; $P < 0.001$ for media versus GRPs; $P < 0.05$ for dead cells versus GRPs; **Fig. 3d**). Transplanted GRPs also significantly delayed forelimb disease onset after hindlimb onset (medium, 7.4 ± 1.2 d; dead cells, 7.3 ± 3.1 d; GRPs, 14.9 ± 5.9 d; $P < 0.001$ for medium versus GRPs; $P < 0.05$ for dead cells versus GRPs; **Fig. 3e**), suggesting that transplantation focally interrupted disease progression from the lumbar to the cervical spinal cord. GRPs did not significantly delay weight decline ($P > 0.05$ for all comparisons; **Fig. 3f**).

We assessed the ability of transplanted GRPs to differentially affect forelimb and hindlimb motor function by grip strength testing. GRPs had no effect on the rate of decline of hindlimb grip strength ($P > 0.05$ for all comparisons; **Fig. 3g**) but significantly slowed the decline in forelimb grip strength ($P < 0.05$ at a number of time points after transplantation; **Fig. 3h**), suggesting that targeting transplantation to the cervical spinal cord results in anatomically specific effects. Transplanted GRPs also slowed the decline in motor performance (**Fig. 3i**).

Previous work showed that seeding of GLT1-overexpressing GRPs on an organotypic slice culture model of motor neuron degeneration results in greater motor neuron preservation than does seeding of wild-type GRPs, an effect mediated by enhanced glutamate uptake[24]. We therefore examined the therapeutic efficacy of GLT1-overexpressing GRPs relative to GRPs. There were no significant differences between rats transplanted with GRPs ($n = 10$) versus GLT-overexpressing GRPs ($n = 9$) in disease duration (GRPs, 21.9 ± 6.1 d; GLT1-overexpressing GRPs, 22.8 ± 3.9 d; $P > 0.05$) or delay to forelimb disease onset after hindlimb onset (GRPs, 14.9 ± 5.9 d; GLT1-overexpressing GRPs, 15.4 ± 4.8 d; $P > 0.05$; **Supplementary Fig. 1** online), two pertinent outcomes that were robustly enhanced by GRP transplantation compared to medium and dead-cell control groups.

To further test the role of graft-derived GLT1 in disease outcome, we generated GLT1-null GRPs from GLT1-null mice[24]. We then transplanted the mouse GLT1-null GRPs into SOD1^{G93A} rat cervical spinal cords using the same approach used for all other transplant groups. Unlike transplants of GRPs and GLT1-overexpressing GRPs, mouse GLT1-null GRPs ($n = 8$) did not extend disease duration (16.6 ± 2.0 d) or prolong the delay to forelimb disease onset after hindlimb onset (7.8 ± 1.4 d; **Supplementary Fig. 1**).

To control for potential species differences in efficacy between rat GRPs and GLT1-overexpressing GRPs and mouse GLT1-null GRPs, we also transplanted GRPs derived from wild-type mice ($n = 6$). Similar to rat-derived GRPs and GLT1-overexpressing GRPs, wild-type mouse GRPs extended disease duration (22.4 ± 3.0 d; data not shown) and prolonged the delay to forelimb disease onset after hindlimb onset (13.3 ± 3.1 d; data not shown). Both wild-type and GLT1-null mouse GRPs survived (31.3 ± 0.07%), differentiated into astrocytes (85.6 ± 1.3%; **Supplementary Fig. 2** online) and migrated selectively along white-matter tracts (5.7 ± 0.2 mm), as detected with the mouse-specific M2 antibody at disease end stage ($n = 3$; GLT1-null GRPs only; **Supplementary Methods**). Quantification of these results showed that the fate of mouse-derived cells was very similar to the results presented earlier for rat-derived GRPs. These findings suggest that there was no significant species-related rejection of mouse-derived GRPs in the rat spinal cord. Combined with the efficacy seen with transplanted wild-type mouse GRPs, these findings suggest that the effects of GLT1-null GRP transplantation were a function of a lack of GLT1, not due to a species-specific phenomenon.

Lastly, we transplanted rat-derived fibroblasts[25] into SOD1^{G93A} rats to test the effect of a non-neural live cell type on disease outcome ($n = 6$) and to control for the potential influence of immune-mediated clearing of dead transplanted cells. As shown by immunofluorescence detection of the transplant marker, human placental alkaline phosphatase, transplanted fibroblasts survived in cervical spinal cord gray matter until disease end stage in all rats (**Supplementary Fig. 1**). Disease duration (14.3 ± 0.8 d) and delay to forelimb disease onset after hindlimb onset (5.8 ± 1.0 d; **Supplementary Fig. 1**) were not significantly different than with media and dead-cell controls.

Phrenic CMAPs and cervical motor neuron loss

Compared to age-matched wild-type rats ($n = 3$; 5.8 ± 0.7 mV), all groups of SOD1^{G93A} rats, regardless of experimental treatment, had

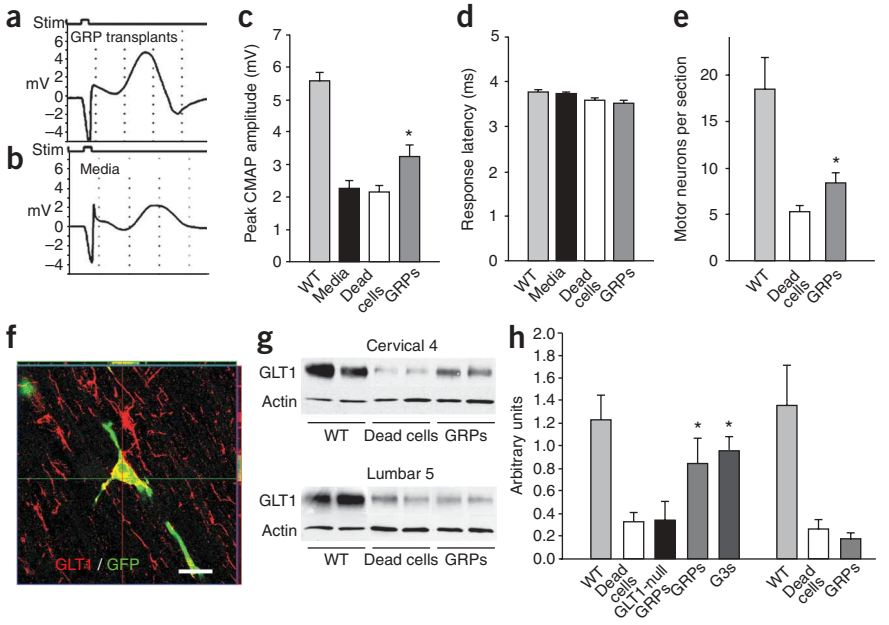

Figure 4 After transplantation into cervical spinal cords of SOD1^{G93A} rats, GRPs partially slowed cervical spinal cord motor neuron and GLT1 protein loss, as well as the decline in phrenic nerve CMAPs. (**a**,**b**) CMAPs were recorded 8 d after hindlimb disease onset. (**c**) A significant increase in peak response amplitude was found in GRP-transplanted rats. Compared to age-matched wild-type (WT) rats, all groups of SOD1^{G93A} rats had significantly reduced peak response amplitudes. (**d**) GRPs had no effect on latency of response. (**e**) Compared to age-matched wild-type rats, all groups of SOD1^{G93A} rats had significantly reduced numbers of cervical spinal cord motor neurons. However, compared to dead-cell controls, GRPs partially rescued cervical motor neurons. (**f**) Grafted GFP^{+} cells continued to express GLT1 protein at disease end stage. (**g**,**h**) Compared to age-matched wild-type rats, all groups of SOD1^{G93A} rats had reduced levels of total GLT1 protein at C4 (**g**). However, compared to rats transplanted with dead cells and GLT1-null GRPs, rats transplanted with GRPs and GLT1-overexpressing GRPs (G3s) had higher levels of total GLT1 levels at C4 (**h**). There was no difference in C4 GLT1 levels between GRPs and GLT1-overexpressing GRPs (**h**). No differences in total GLT1 protein among any of the treatment groups were found at L5 (**g**,**h**, right 3 bars), indicating that focal transplantation resulted in changes in transporter protein levels only at cervical regions and that disease progression was likely to be unchanged at other nontargeted areas. Scale bars, 20 μm. Error bars indicate s.e.m. Asterisks indicate significance ($P < 0.05$) in comparison with dead cells.

significantly lower peak response amplitudes of phrenic nerve compound muscle action potentials (CMAPs), a functional electrophysiological measure of diaphragm function[21]. Compared to media ($n = 10$) or dead cell ($n = 8$) controls, GRP transplantation ($n = 8$) slowed the decline in CMAP amplitudes. We recorded CMAPs (**Fig. 4a**,**b**) 8 d after hindlimb disease onset and observed a significant increase (**Fig. 4c**) in peak response amplitude in GRP-transplanted rats (media, 2.25 ± 0.8 mV; dead cells, 2.1 ± 0.6 mV; GRPs, 3.2 ± 1.0 mV; $P < 0.05$ for media and dead cells versus GRPs). Transplanted cells had no effect on response latency (medium, 3.7 ± 0.1 ms; dead cells, 3.6 ± 0.2 ms; GRPs, 3.5 ± 0.2 ms; $P > 0.05$; **Fig. 4d**).

We next quantified the neuroprotective effect of GRPs on cervical spinal cord motor neuron loss (**Supplementary Methods**). Compared to age-matched wild-type rats ($n = 3$; 18.5 ± 5.9 motor neurons per section; **Fig. 4e**), all groups of SOD1^{G93A} rats, regardless of experimental treatment, had significantly lower numbers of cervical spinal cord motor neurons. Compared to dead cells ($n = 9$), GRPs ($n = 5$) partially rescued (a 47% increase) cervical motor neurons (dead cells, 5.3 ± 2.0; GRPs, 7.8 ± 3.2; $P < 0.05$), which was likely to account for the benefits observed in functional and behavioral measures.

No differences were noted between GRPs, GLT-overexpressing GRPs ($n = 5$) and wild-type mouse GRPs ($n = 5$) with respect to CMAP amplitudes (GRPs, data not shown; GLT1-overexpressing GRPs, 3.5 ± 0.3 mV; wild-type mouse GRPs, 3.4 ± 0.4 mV; $P > 0.05$ for all comparisons) or between GRPs and GLT-overexpressing GRPs ($n = 4$) with respect to cervical motor neuron counts (GRPs, data not shown; GLT1-overexpressing GRPs, 9.4 ± 2.0 motor neurons per section; $P > 0.05$).

Partial preservation of cervical spinal cord GLT1 levels

Previous work has shown a role for loss of astroglial glutamate transport in the progression of ALS[26]. Preservation of GLT1 levels, through either transplant-derived replacement or prevention of loss from host cells, provides one possible mechanism for astrocyte-specific transplant efficacy. Grafted GRPs continued to express GLT1 at endstage (**Fig. 4f**). We therefore measured levels of GLT1 protein in cervical spinal cords of rats 8 d after hindlimb onset (**Fig. 4g** and **Supplementary Methods**). Compared to age-matched wild-type rats ($n = 2$; 1.22 ± 0.23 arbitrary units; **Fig. 4h**), all groups of SOD1^{G93A} rats, regardless of experimental treatment, had lower levels of total GLT1 protein at the C4 cervical spinal cord level. Transplantation of GRPs attenuated the loss of total GLT1 levels focally in the spinal cord at C4 ($n = 3$ per group; dead cells, 0.32 ± 0.09; GRPs, 0.84 ± 0.23; $P < 0.05$; **Fig. 4h**) and C6 (data not shown). We found no differences among treatment groups in levels of total GLT1 when lumbar level 5 tissue was tested (wild type, $n = 2$, 1.36 ± 0.50 arbitrary units; dead cells, $n = 5$, 0.26 ± 0.18; GRPs, $n = 5$, 0.17 ± 0.11; $P > 0.05$ for dead cells versus GRPs; **Fig. 4h**), although all SOD1^{G93A} rat groups had lower levels than did age-matched wild-type rats.

Notably, although GLT1-overexpressing GRPs have much higher expression levels of GLT1 *in vitro* than do GRPs[24], total GLT1 levels in C4 spinal cord transplanted with GLT1-overexpressing GRPs were not significantly higher than in GRP-transplanted tissue ($n = 3$; 0.95 ± 0.12 arbitrary units; $P > 0.05$ for GLT1-overexpressing GRPs vs. GRPs; **Fig. 4h**). Unlike transplants of GRPs and GLT1-overexpressing GRPs, GLT1-null GRPs ($n = 3$) did not maintain GLT1 expression. There was no significant difference in levels of GLT1 in the cervical spinal cord between dead-cell controls and transplanted GLT1-null GRPs ($n = 3$; 0.33 ± 0.17 arbitrary units; $P < 0.05$ for GLT1-null GRPs versus GRPs; $P > 0.05$ for GLT1-null GRPs versus dead cells; **Fig. 4h**). These results suggest that graft-derived GLT1 accounts for most of the preservation of cervical spinal cord GLT1 levels after transplantation. Taken together, these results provide at least one plausible benefit of astrocyte replacement, although other astrocytic mechanisms may also be relevant.

No changes in growth factors but reduced microgliosis

The transplanted GRPs may also have promoted therapeutic benefits through mechanisms other than increased GLT1 levels. For example, transplanted GRPs could have released trophic factors, resulting in neuroprotection. We therefore conducted enzyme-linked

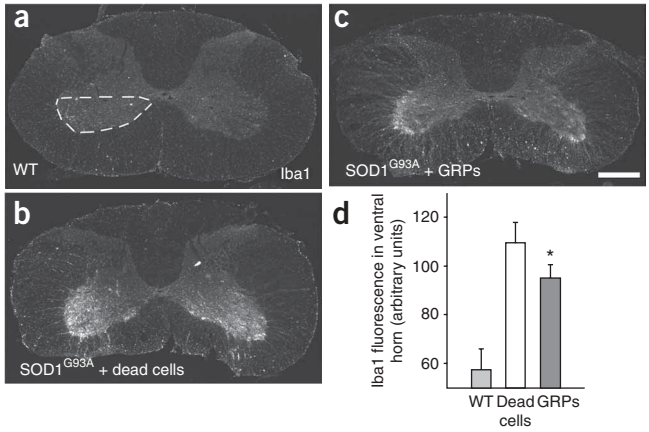

Figure 5 GRP transplants decreased ventral horn microgliosis. (**a**–**c**) Compared to wild-type (WT) spinal cords (**a**), there was a significantly elevated Iba1$^+$ microglial response specifically in the ventral gray matter of SOD1^{G93A} rats with injections of dead cells (**b**) or GRPs (**c**). (**d**) Quantification of the Iba1 response in ventral gray matter (region within dotted line in **a**) revealed that microgliosis was significantly reduced in GRP-transplanted animals compared to dead-cell controls ($^*P < 0.05$). Scale bar, 200 μm. Error bars indicate s.e.m.

immunosorbent assays of brain-derived neurotrophic factor (BDNF), insulin-like growth factor 1 (IGF-1) and vascular endothelial growth factor (VEGF) in cervical spinal cord parenchyma at the levels transplanted with GRPs (**Supplementary Methods**). The beneficial roles of these trophic factors on disease outcome in mutant SOD1–expressing rodent models have been previously shown[27]. We did not observe significant differences in levels of VEGF (wild type, 46.3 ± 15.2 pg ml^{-1}; dead cells, 48.1 ± 1.3 pg ml^{-1}; GRPs, 61.9 ± 11.2 pg ml^{-1}; $n = 3$ per group; $P > 0.05$ for all comparisons), BDNF (wild type, 3.6 ± 0.7 pg ml^{-1}; dead cells, 5.8 ± 1.7 pg ml^{-1}; GRPs, 4.6 ± 1.2 pg ml^{-1}; $n = 3$ per group; $P > 0.05$ for all comparisons) or IGF-1 (wild type, 142.6 ± 29.8 pg ml^{-1}; dead cells, 150.7 ± 23.9 pg ml^{-1}; GRPs, 172.1 ± 18.7 pg ml^{-1}; $n = 3$ per group; $P > 0.05$ for all comparisons; **Supplementary Fig. 3** online) between any of the groups studied.

We examined the inflammatory response by analyzing the microglial marker Iba1 in age-matched cervical spinal cords from dead cell– and GRP-transplanted rats (**Supplementary Methods**). Immunohistochemistry revealed that compared to wild-type spinal cords ($n = 4$; **Fig. 5a**), there was a significantly elevated microglial response specifically in the ventral gray matter of both dead cell control ($n = 6$; **Fig. 5b**) and GRP-transplanted ($n = 4$; **Fig. 5c**) SOD1^{G93A} rats. However, the response was significantly lower in GRP-transplanted rats (wild-type, 58.0 ± 4.1 arbitrary units; dead cell, 110.0 ± 3.4; GRPs, 95.4 ± 2.8; $P < 0.05$; **Fig. 5d**). The effects of GRP transplantation on disease progression after symptomatic onset in this study are similar to previous results of a study in which mutant SOD1 expression was selectively removed from microglia[7] and may be attributed in part to a muted microglial response in the cervical spinal cord.

DISCUSSION

The neuroprotective effects observed in this study indicate the feasibility and efficacy of focal transplantation-based astrocyte replacement for ALS and show that targeted multisegmental cell delivery to the cervical spinal cord is a promising therapeutic strategy, particularly because of its relevance to addressing the respiratory compromise associated with ALS. Over the last 10 years, accumulating data have implicated non-neuronal cells in the pathogenesis of neuronal degeneration in ALS. From the earliest studies of functional abnormalities in ALS astrocytes[18,28], to the more recent studies in chimeric mice[8], the aberrant function of cells including microglia[7] and astroglia[13] that surround motor neuron somas and dendrites has seemed to contribute to disease progression. Chimeric mutant SOD1 models suggest that increasing the proportion of healthy wild-type non-neuronal cells is inversely related to measures of disease severity such as animal survival[8], similar to the effects of GRP transplantation observed in the present study. In these chimeric mice, the presence of wild-type non-neuronal cells (probably astrocytes and microglia) in the spatial vicinity of mutant SOD1–expressing motor neurons prevented pathological changes in these neurons. More recent studies show that the reduction of mutant SOD1 selectively from astrocytes in LoxSOD1^{G37R}/GFAP-Cre$^+$ mice results in a prolongation of disease duration but has no effects on disease onset[13]. These results suggest a particular role for astrocytes in later progression of disease. Together, these studies suggest that replacement of abnormal astroglia—or enrichment of healthy astroglia—with normal functioning precursors could be one approach to focally altering the microenvironment around motor neurons.

Dysfunction of astrocyte glutamate transport, specifically GLT1 (EAAT2), is found in humans with ALS and in animal models of ALS[6,18] and may be a contributing factor in disease progression. Loss of this astroglial protein is known to cause excitotoxic motor neuron degeneration[15]. Furthermore, ALS astrocytes alter the expression of dendritic glutamate (AMPA) receptors in motor neurons, also making them more susceptible to excitotoxicity. Small-molecule drug screening for agents that enhance glial glutamate transporter function shows that increasing astroglial GLT1 can be beneficial in ALS models[29]. Several more recent *in vitro* studies of immature ALS rodent astrocytes also suggest abnormal properties resulting in motor neuron cell death[9,11], although the exact mechanisms remain unknown. Thus, any approach to offset or replace altered astroglial function—especially in mature astrocytes—may be of therapeutic benefit.

In the present study, transplanted GRPs were able to partially prevent loss of total tissue GLT1 levels in the cervical cord, thereby targeting one important, and ALS-relevant, function of astrocytes. The finding that GLT1-null GRPs did not have any effects on behavioral measures or rat survival also suggests that glutamate-relevant pathways contribute to the cascade of events leading to cell death in this model, and that the focal beneficial effects of GRP transplantation could be explained, at least in part, by increases in glutamate transporter expression. Although disease duration is extended by reducing mutant SOD1 from astrocytes in the LoxSOD1^{G37R}/GFAP-Cre$^+$ mice, GLT1 loss in lumbar spinal cord sections does not depend on the presence of mutant SOD1 in astrocytes[13]. GLT1 loss may instead be related to non-cell-autonomous damage to astrocytes from SOD1 synthesis by other cells. Alternatively, alterations in neuron-astrocyte communication, as a result of SOD1-mediated neuronal injury, could be responsible. Several explanations could account for the discrepancy between our observations in the present study and those of the previous study[13]. These include the anatomical location of tissue sampling (both cervical and lumbar spinal cord versus lumbar only, respectively), time frame of sampling (at a specific time point during disease course versus end stage) and contributions of GLT1 loss to death in different species carrying different SOD1 mutations that result in differences in disease course itself (disease course $<$180 d in the SOD1^{G93A} rat model versus $>$375 d in the SOD1^{G37R} mouse model). Finally, it is also possible that the increases in GLT1 that we observed in our model may represent only one of several related pathways relevant to astrocytic influences on disease progression. The lack of further increases in behavioral

and neuroprotective measures from the transplantation of GLT1-overexpressing GRPs may be related to the observation that increases in GLT1 levels were relatively small compared to previous *in vitro* studies[24] and *in vivo* drug studies[29].

Astrogliosis with GFAP upregulation is a central feature of ALS and SOD1 pathology, and previous studies have noted that some protective molecules downregulate GFAP expression in ALS models[30]. We did not observe any detrimental effects on disease after introduction of GFAP$^+$ GRP-derived astrocytes. These results suggest that astrogliosis is reflected not only by increases in GFAP expression, but also by other astrocyte factors that may influence disease progression. Furthermore, the direct effect of astrogliosis itself is unclear, as reactive astrocytes also have important protective roles in other CNS injury paradigms[31].

Transplantation of neural precursor cells offers a strategy for slowing neurodegenerative disease progression and promoting recovery of function, because engrafted cells have the potential of replacing lost or dysfunctional neurons and glia. Previous neural precursor transplantation studies in motor neuronopathies have focused mostly on motor neuron replacement[32–35]; however, this is a challenging strategy for neurodegenerative diseases because of problems associated with motor neuron differentiation, establishment of appropriate circuitry with host neurons, and extension to and connectivity with musculature.

Other transplantation strategies not based on motor neuron replacement, including those with enhanced trophic factor production, also show promise in ALS models[36–47]. When transplanted into the lumbar spinal cords of SOD1^{G93A} rats, human neural progenitor cells that overexpress glial cell line–derived neurotrophic factor provide some, albeit limited, neuroprotection[48,49]. These transplants provide a neuroprotective effect on motor neuron survival but do not promote efficacy with respect to improved hindlimb motor performance and animal survival, possibly because of a lack of astrocyte differentiation *in vivo*. Our study did not suggest that there is a pattern of significant increases in VEGF, IGF-1 or BDNF secretion to account for the observed pathological or behavioral phenotypes. However, it is possible that at the cellular level, some neurotrophic factor secretion had a role in the efficacy of GRPs but was not appreciated in the whole-tissue analysis of the cervical spinal cord in this study.

These results serve as a proof of principle that stem cell transplantation–based astrocyte replacement is feasible and a potentially viable option for ALS therapy. Delivery of glial progenitors to the cervical spinal cord targets key motor neuron pools that ultimately affect survival in ALS patients, and respiratory measures remain the most reliable for use in ALS clinical trials.

Glial precursors are particularly promising candidates for astrocyte replacement because of their robust survival, efficient astrocytic differentiation and lack of tumor formation. Whereas more immature cell classes such as multipotent neural stem cells and pluripotent embryonic stem cells are desirable sources for transplant derivation, the present study suggests that the use of more mature lineage-restricted progenitors would be an optimal strategy for achieving targeted phenotypic replacement.

METHODS

GRP transplantation. GRPs, GLT1-overexpressing GRPs, GLT1-null GRPs, freeze-thawed dead GRPs and unmodified rat fibroblasts[25] were suspended at a concentration of 7.5×10^4 cells μl^{-1} in basal medium. Rats were immune-suppressed with cyclosporine A (10 mg kg^{-1}; Sandoz Pharmaceuticals) and given transplants at 90 d of age. Seven treatment groups were used: wild-type rat GRPs, GLT1-overexpressing rat GRPs, GLT1-null mouse GRPs, wild-type mouse GRPs, rat fibroblasts, dead wild-type rat GRPs and medium only. Each rat received six grafts (bilaterally at C4, C5 and C6) of 1.5×10^5 cells (in 2 µl basal medium) into the ventral horn. Cells were delivered using a 10-µl Gastight syringe (Hamilton) with an attached 30-gauge 45° beveled needle (Hamilton). The injection pipette was secured to a manual micromanipulator (World Precision Instruments) attached to an 80° tilting base. The tip was lowered to a depth of 1.5 mm below the surface of the cord and was held in place for 2 min before and after cell injection. Cells were delivered under the control of a microsyringe pump controller (World Precision Instruments) at a rate of 0.5 µl min^{-1}. The care and treatment of animals in all procedures was conducted with the approval of the Johns Hopkins University IACUC.

Hindlimb and forelimb grip strength. Rats were weighed and all behavioral data collected 1 week before transplantation and then twice weekly until end stage. Hindlimb and forelimb muscle grip strengths were separately determined using a grip strength meter (DFIS-2 series digital force gauge, Columbus Instruments).

Disease onset. Hindlimb and forelimb disease onsets were assessed individually for each rat by a 20.0% loss in hindlimb or forelimb grip strength relative to each rat's own baseline grip strength level.

End-stage analysis. To determine disease end stage in a reliable and ethical fashion, end stage was defined by the inability of rats to right themselves within 30 s when placed on their sides.

Disease duration. Overall onset of disease was determined by hindlimb grip strength, as hindlimb deficits are the first clinical symptoms observed in most rats. Disease duration was measured as time between hindlimb disease onset and disease end stage. All SOD1^{G93A} rats were included in overall survival, disease onset and grip strength analyses; however, rats that showed forelimb onset before hindlimb onset (approximately 10% of SOD1^{G93A} rats) were excluded from analysis of disease duration and delay of forelimb onset after hindlimb onset.

Forelimb and hindlimb combined motor score. A five-point scale was used to simultaneously assess forelimb and hindlimb function, as previously described[47].

Compound muscle action potential recordings. Phrenic nerve conduction studies were conducted[21] on anesthetized rats with stimulation (0.5-ms single stimulus and 1-Hz supramaximal pulses) at the neck through near-nerve needle electrodes placed 0.5 cm apart along the phrenic nerve. Recordings were obtained by a surface strip along the costal margin, and CMAP amplitudes were measured from baseline to peak. Recordings across the nerve segment were made using an ADI PowerLab 8SP stimulator and Bio Amp amplifier (ADInstruments), followed by computer-assisted data analysis (Scope 3.5.6 software; ADInstruments). Distal motor latency of evoked potentials included duration of nerve conduction between stimulating and recording electrodes plus time of synaptic transmission.

Statistical analysis. Kaplan-Meier analysis of the SOD1^{G93A} rats was conducted using the statistical software SigmaStat (SAS Software) to analyze survival, disease onset and duration data. Weight and grip strength results were subjected to analysis of variance. In some cases, Student's t test was used to compare data between groups of rats. All data are presented as mean ± s.e.m., and significance level was set at $P \leq 0.05$.

Note: Supplementary information is available on the Nature Neuroscience website.

ACKNOWLEDGMENTS

We thank all members of the Maragakis and Rothstein labs for helpful discussion and K. Tanaka for providing GLT1-null mice. This work was supported by the Robert Packard Center for ALS Research (to N.J.M.), the ALS Association (to N.J.M.) and the National Institutes of Health (F32-NS059155 to A.C.L., R01-NS33958 to J.D.R. and R01-NS41680 to J.D.R. and N.J.M.).

AUTHOR CONTRIBUTIONS

A.C.L. designed and conducted the experiments, analyzed the data, prepared the figures and wrote the manuscript. N.J.M. supervised the project and participated in designing experiments and writing the manuscript. M.S.R. and J.D.R.

participated in designing experiments and writing the manuscript. B.R., A.C.P. and C.D. conducted experiments.

COMPETING INTERESTS STATEMENT

The authors declare competing financial interests: details accompany the full-text HTML version of the paper at www.nature.com/natureneuroscience/.

Published online at http://www.nature.com/natureneuroscience/

1. Bruijn, L.I., Miller, T.M. & Cleveland, D.W. Unraveling the mechanisms involved in motor neuron degeneration in ALS. *Annu. Rev. Neurosci.* **27**, 723–749 (2004).
2. Rosen, D.R. *et al.* Mutations in Cu/Zn superoxide dismutase gene are associated with familial amyotrophic lateral sclerosis. *Nature* **362**, 59–62 (1993).
3. Bruijn, L.I. *et al.* ALS-linked SOD1 mutant G85R mediates damage to astrocytes and promotes rapidly progressive disease with SOD1-containing inclusions. *Neuron* **18**, 327–338 (1997).
4. Gurney, M.E. *et al.* Motor neuron degeneration in mice that express a human Cu, Zn superoxide dismutase mutation. *Science* **264**, 1772–1775 (1994).
5. Wong, P.C. *et al.* An adverse property of a familial ALS-linked SOD1 mutation causes motor neuron disease characterized by vacuolar degeneration of mitochondria. *Neuron* **14**, 1105–1116 (1995).
6. Howland, D.S. *et al.* Focal loss of the glutamate transporter EAAT2 in a transgenic rat model of SOD1 mutant–mediated amyotrophic lateral sclerosis (ALS). *Proc. Natl. Acad. Sci. USA* **99**, 1604–1609 (2002).
7. Boillee, S. *et al.* Onset and progression in inherited ALS determined by motor neurons and microglia. *Science* **312**, 1389–1392 (2006).
8. Clement, A.M. *et al.* Wild-type non-neuronal cells extend survival of SOD1 mutant motor neurons in ALS mice. *Science* **302**, 113–117 (2003).
9. Di Giorgio, F.P., Carrasco, M.A., Siao, M.C., Maniatis, T. & Eggan, K. Non-cell autonomous effect of glia on motor neurons in an embryonic stem cell–based ALS model. *Nat. Neurosci.* **10**, 608–614 (2007).
10. Lino, M.M., Schneider, C. & Caroni, P. Accumulation of SOD1 mutants in postnatal motoneurons does not cause motoneuron pathology or motoneuron disease. *J. Neurosci.* **22**, 4825–4832 (2002).
11. Nagai, M. *et al.* Astrocytes expressing ALS-linked mutated SOD1 release factors selectively toxic to motor neurons. *Nat. Neurosci.* **10**, 615–622 (2007).
12. Pramatarova, A., Laganiere, J., Roussel, J., Brisebois, K. & Rouleau, G.A. Neuron-specific expression of mutant superoxide dismutase 1 in transgenic mice does not lead to motor impairment. *J. Neurosci.* **21**, 3369–3374 (2001).
13. Yamanaka, K. *et al.* Astrocytes as determinants of disease progression in inherited amyotrophic lateral sclerosis. *Nat. Neurosci.* **11**, 251–253 (2008).
14. Pekny, M. & Nilsson, M. Astrocyte activation and reactive gliosis. *Glia* **50**, 427–434 (2005).
15. Rothstein, J.D. *et al.* Knockout of glutamate transporters reveals a major role for astroglial transport in excitotoxicity and clearance of glutamate. *Neuron* **16**, 675–686 (1996).
16. Rothstein, J.D. *et al.* Localization of neuronal and glial glutamate transporters. *Neuron* **13**, 713–725 (1994).
17. Maragakis, N.J. & Rothstein, J.D. Mechanisms of disease: astrocytes in neurodegenerative disease. *Nat. Clin. Pract. Neurol.* **2**, 679–689 (2006).
18. Rothstein, J.D., Van Kammen, M., Levey, A.I., Martin, L.J. & Kuncl, R.W. Selective loss of glial glutamate transporter GLT-1 in amyotrophic lateral sclerosis. *Ann. Neurol.* **38**, 73–84 (1995).
19. Rao, M.S. & Mayer-Proschel, M. Glial-restricted precursors are derived from multipotent neuroepithelial stem cells. *Dev. Biol.* **188**, 48–63 (1997).
20. Rao, M.S., Noble, M. & Mayer-Proschel, M. A tripotential glial precursor cell is present in the developing spinal cord. *Proc. Natl. Acad. Sci. USA* **95**, 3996–4001 (1998).
21. Llado, J. *et al.* Degeneration of respiratory motor neurons in the SOD1 G93A transgenic rat model of ALS. *Neurobiol. Dis.* **21**, 110–118 (2006).
22. Tankersley, C.G., Haenggeli, C. & Rothstein, J.D. Respiratory impairment in a mouse model of amyotrophic lateral sclerosis. *J. Appl. Physiol.* **102**, 926–932 (2007).
23. Matsumoto, A. *et al.* Disease progression of human SOD1 (G93A) transgenic ALS model rats. *J. Neurosci. Res.* **83**, 119–133 (2006).
24. Maragakis, N.J. *et al.* Glial restricted precursors protect against chronic glutamate neurotoxicity of motor neurons *in vitro*. *Glia* **50**, 145–159 (2005).
25. Mitsui, T., Fischer, I., Shumsky, J.S. & Murray, M. Transplants of fibroblasts expressing BDNF and NT-3 promote recovery of bladder and hindlimb function following spinal contusion injury in rats. *Exp. Neurol.* **194**, 410–431 (2005).
26. Maragakis, N.J. & Rothstein, J.D. Glutamate transporters: animal models to neurologic disease. *Neurobiol. Dis.* **15**, 461–473 (2004).
27. Federici, T. & Boulis, N.M. Gene-based treatment of motor neuron diseases. *Muscle Nerve* **33**, 302–323 (2006).
28. Rothstein, J.D., Martin, L.J. & Kuncl, R.W. Decreased glutamate transport by the brain and spinal cord in amyotrophic lateral sclerosis. *N. Engl. J. Med.* **326**, 1464–1468 (1992).
29. Rothstein, J.D. *et al.* Beta-lactam antibiotics offer neuroprotection by increasing glutamate transporter expression. *Nature* **433**, 73–77 (2005).
30. Kiaei, M., Kipiani, K., Chen, J., Calingasan, N.Y. & Beal, M.F. Peroxisome proliferator-activated receptor-gamma agonist extends survival in transgenic mouse model of amyotrophic lateral sclerosis. *Exp. Neurol.* **191**, 331–336 (2005).
31. Sofroniew, M.V. Reactive astrocytes in neural repair and protection. *Neuroscientist* **11**, 400–407 (2005).
32. Deshpande, D.M. *et al.* Recovery from paralysis in adult rats using embryonic stem cells. *Ann. Neurol.* **60**, 32–44 (2006).
33. Harper, J.M. *et al.* Axonal growth of embryonic stem cell–derived motoneurons *in vitro* and in motoneuron-injured adult rats. *Proc. Natl. Acad. Sci. USA* **101**, 7123–7128 (2004).
34. Kerr, D.A. *et al.* Human embryonic germ cell derivatives facilitate motor recovery of rats with diffuse motor neuron injury. *J. Neurosci.* **23**, 5131–5140 (2003).
35. Wu, P. *et al.* Region-specific generation of cholinergic neurons from fetal human neural stem cells grafted in adult rats. *Nat. Neurosci.* **5**, 1271–1278 (2002).
36. Aebischer, P. *et al.* Gene therapy for amyotrophic lateral sclerosis (ALS) using a polymer encapsulated xenogenic cell line engineered to secrete hCNTF. *Hum. Gene Ther.* **7**, 851–860 (1996).
37. Aebischer, P. *et al.* Intrathecal delivery of CNTF using encapsulated genetically modified xenogeneic cells in amyotrophic lateral sclerosis patients. *Nat. Med.* **2**, 696–699 (1996).
38. Corti, S. *et al.* Wild-type bone marrow cells ameliorate the phenotype of SOD1-G93A ALS mice and contribute to CNS, heart and skeletal muscle tissues. *Brain* **127**, 2518–2532 (2004).
39. Corti, S. *et al.* Neural stem cells LewisX$^+$ CXCR4$^+$ modify disease progression in an amyotrophic lateral sclerosis model. *Brain* **130**, 1289–1305 (2007).
40. Garbuzova-Davis, S. *et al.* Intraspinal implantation of hNT neurons into SOD1 mice with apparent motor deficit. *Amyotroph. Lateral Scler. Other Motor Neuron Disord.* **2**, 175–180 (2001).
41. Garbuzova-Davis, S. *et al.* Positive effect of transplantation of hNT neurons (NTera 2/D1 cell line) in a model of familial amyotrophic lateral sclerosis. *Exp. Neurol.* **174**, 169–180 (2002).
42. Garbuzova-Davis, S. *et al.* Intravenous administration of human umbilical cord blood cells in a mouse model of amyotrophic lateral sclerosis: distribution, migration and differentiation. *J. Hematother. Stem Cell Res.* **12**, 255–270 (2003).
43. Hemendinger, R. *et al.* Sertoli cells improve survival of motor neurons in SOD1 transgenic mice, a model of amyotrophic lateral sclerosis. *Exp. Neurol.* **196**, 235–243 (2005).
44. Llado, J., Haenggeli, C., Maragakis, N.J., Snyder, E.Y. & Rothstein, J.D. Neural stem cells protect against glutamate-induced excitotoxicity and promote survival of injured motor neurons through the secretion of neurotrophic factors. *Mol. Cell. Neurosci.* **27**, 322–331 (2004).
45. Martin, L.J. & Liu, Z. Adult olfactory bulb neural precursor cell grafts provide temporary protection from motor neuron degeneration, improve motor function and extend survival in amyotrophic lateral sclerosis mice. *J. Neuropathol. Exp. Neurol.* **66**, 1002–1018 (2007).
46. Xu, L. *et al.* Human neural stem cell grafts ameliorate motor neuron disease in SOD-1 transgenic rats. *Transplantation* **82**, 865–875 (2006).
47. Yan, J. *et al.* Combined immunosuppressive agents or CD4 antibodies prolong survival of human neural stem cell grafts and improve disease outcomes in amyotrophic lateral sclerosis transgenic mice. *Stem Cells* **24**, 1976–1985 (2006).
48. Klein, S.M. *et al.* GDNF delivery using human neural progenitor cells in a rat model of ALS. *Hum. Gene Ther.* **16**, 509–521 (2005).
49. Suzuki, M. *et al.* GDNF secreting human neural progenitor cells protect dying motor neurons, but not their projection to muscle, in a rat model of familial ALS. *PLoS ONE* **2**, e689 (2007).